

A Monte Carlo Technique to Investigate Signal Delays of Advanced Si BJT's up to High Currents

Pierpaolo Palestri, Luca Selmi, Fred Hurkx* and J.Slotboom*
 DIEGM, Via delle Scienze 208, 33100 Udine, Italy
 Fax:+39-0432-558251 email: luca.selmi@diegm.uniud.it
 * Philips Research Laboratories, Eindhoven, The Netherlands

Abstract— We present a new Monte Carlo technique to investigate the signal delay of advanced BJTs featuring relevant non-local effects. The method is suited to analyze base and collector signal delays in presence of significant non-equilibrium transport effects and up to high currents, and to verify the physical meaning and applicability of delay expressions for compact models.

I. INTRODUCTION

The collector signal delay is becoming an increasingly important ingredient of the overall signal delay of advanced Si and Si-Ge BJT's and a limiting factor for achieving high cut-off frequencies [1]. This delay contribution is strongly affected by non-equilibrium transport and velocity overshoot [1], [2], [3]. Hence, drift-diffusion analysis is inaccurate, while spurious velocity overshoot [4] and difficult convergence limit the applicability of hydrodynamic approaches. The Monte Carlo method (MC) provides an alternative mean to tackle these problems in the framework of an accurate description of high field transport and in this paper we describe a Monte Carlo based technique to study base and collector signal delays, as well as its application to advanced BJT structures.

II. SIMULATION METHOD

The simulation algorithm (whose flowchart is illustrated in Fig. 1), loops self-consistently between the Poisson equation and MC electron transport, while holes are treated classically in the Poisson solver. The MC part implements a non-parabolic, anisotropic band model, carrier multiplication in phase space and the most relevant scattering mechanisms, but more accurate full band approaches can be used as well. In the simulations, a constant electron current density ($J_{n,0}$) is injected at the top of the emitter base potential barrier (located at $x = 0$). When steady state is reached, a double pulse with zero dc value is added to $J_{n,0}$ (as shown in Fig. 2) and simulated self-consistently with a short time step ($\Delta t \leq 1$ fs), until steady state is reached again. To reduce statistical noise [5], especially in the highly doped regions, $J_n(t, x)$ is computed from charge variations with a new estimator that exploits the continuity equation and the knowledge of $J_n(0, t)$. At the

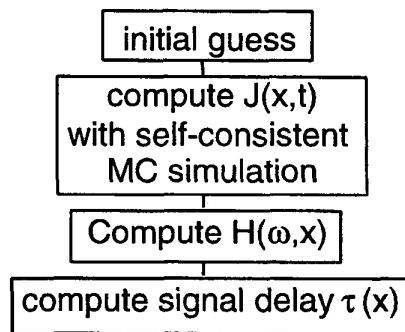


Fig. 1. Flowchart of the simulation procedure.

end of the simulation we compute the small signal transfer function up to x as:

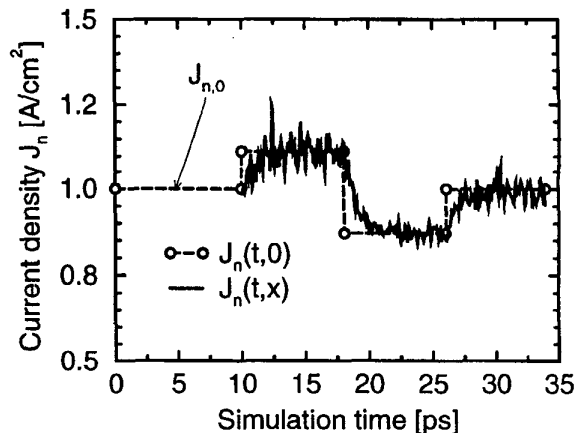


Fig. 2. Typical current density waveforms $J_n(t, x)$ during the self consistent transient simulation at left edge of the base (dashed) and in the middle of the epi layer (solid).

$$H(\omega, x) \triangleq \frac{\bar{J}_n(\omega, x)}{\bar{J}_n(\omega, 0)} = \frac{\mathcal{F}[J_n(t, x) - J_{n,0}]}{\mathcal{F}[J_n(t, 0) - J_{n,0}]} \quad (1)$$

where $\bar{J}_n(\omega, x)$ is the small signal current at x in the frequency domain and \mathcal{F} is the Discrete Fourier Transform operator.

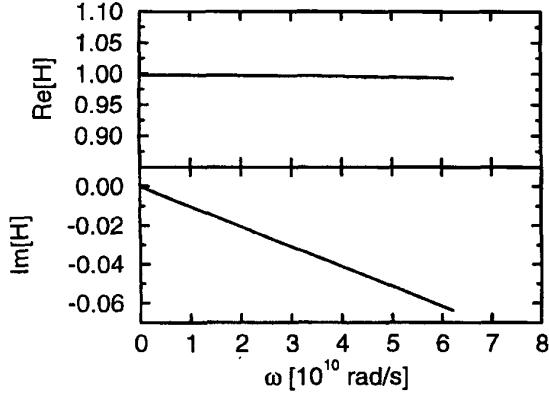


Fig. 3. Real and imaginary part of the small signal transfer function $H(\omega, x)$ for a point in the middle of the epi layer of a typical BJT device. As expected, $Re[H] = 1$ and $Im[H]$ is linear in ω .

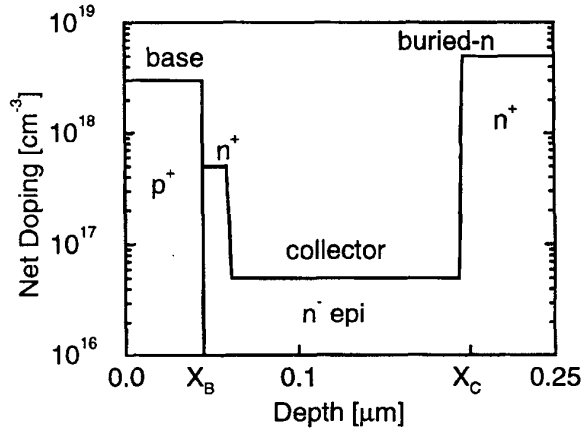


Fig. 4. Schematic representation of the doping profile of the simulated devices.

The signal delay $\tau(x)$ is derived from the low frequency expansion:

$$H(\omega, x) \simeq 1 - j\omega\tau(x) \quad (2)$$

The validity of this expansion is demonstrated in Fig. 3, reporting typical real ($Re[H]$) and imaginary ($Im[H]$) parts of $H(\omega, x)$ for a point inside the epi-layer of a conventional BJT biased at low current. As expected from Eq. 2, $Re[H] = 1$ while $Im[H]$ is a linear function of ω , thus allowing a simple extraction of $\tau(x)$.

III. SIGNAL DELAY AT LOW CURRENT

To demonstrate the method we study BJT's as those of [6], [7], [8], [9] i.e. featuring a thin heavily doped n-type layer adjacent to base collector junction that, if properly designed, reduces boron penetration from the base and improves the cut-off frequency without deteriorating the

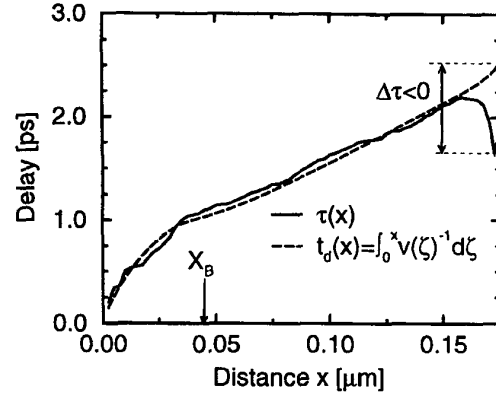


Fig. 5. Solid line: signal delay along the base and collector computed with the method of this work. Dashed line: transit time of the same structure computed from the MC velocity profile. Bias current is $J_{n,0} = 1 \cdot 10^3$ A/cm².

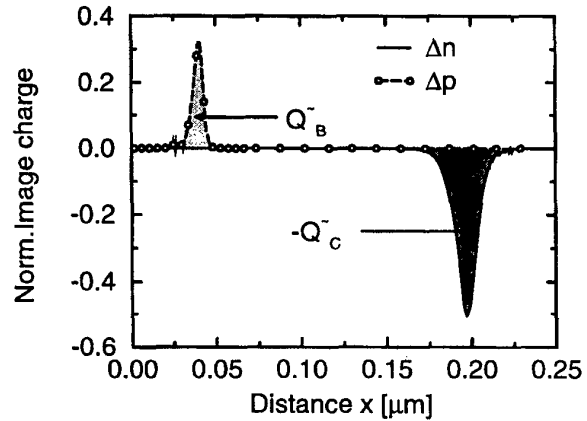


Fig. 6. Normalized electron and hole image charges induced by a Dirac's delta like electron pulse located at $x = 0.15$ μm in the BJT of Fig. 5. The area below the curves is proportional to \tilde{Q}_C^- and \tilde{Q}_B^- , respectively.

breakdown voltage [9] (see Fig. 4). These devices are especially difficult to simulate because the non uniform field generated by the high dope layer gives rise to substantial non-local effects at low as well as high current [8], [9]. Fig. 5 compares the signal delay $\tau(x)$ from MC simulations of one such device at low current with the transit time:

$$t_d(x) = \int_0^x \frac{d\xi}{v(\xi)} \quad (3)$$

where $v(\xi)$ is the MC velocity. Good agreement is found up to the end of the collector space charge region (SCR), where v drops, hence $t_d(x)$ tends to diverge, while $\tau(x)$ decreases, eventually yielding $\tau < t_d$.

This is because the traveling pulse forces some electrons

to leave the right edge of the collector space charge region (SCR). A positive image charge ($\tilde{Q}_C > 0$) is thus generated at the collector right edge before the pulse actually reaches it [10], [11]. This is exemplified in Fig. 6, reporting the image charge corresponding to a Dirac's δ -like charge distribution located in the middle of the epi layer. Since it can be shown with the small signal continuity equation (see, e.g.[12]) that:

$$\tau(x) = -\frac{\tilde{Q}_n(x)}{\tilde{J}_n(0)} \quad (4)$$

where:

$$\tilde{Q}_n(x) = \int_0^x \tilde{q}_n(\xi) d\xi \quad (5)$$

and \tilde{q}_n is the small signal electron charge fluctuation, the incremental delay associated to \tilde{Q}_C :

$$\Delta\tau = -\frac{\tilde{Q}_C}{\tilde{J}_n(0)} \quad (6)$$

is negative. The image charge at the base edge of the SCR (\tilde{Q}_B), instead, is due to holes; hence it does not contribute to the electron signal delay τ .

IV. SIGNAL DELAY AT HIGH CURRENT

As $J_{n,0}$ increases, and the maximum cut-off frequency (f_T) is approached, high injection pushes the field towards the buried n^+ layer, thus giving rise to a narrow field spike and highly non-uniform velocity profile, as clearly visible in Fig. 7.

Quasi-neutrality in the high injection region adjacent to the BC junction forces both electrons and holes to contribute to the image charge \tilde{Q}_B induced by electrons moving in the SCR, that is:

$$\tilde{Q}_B = \tilde{Q}_{B,n} + \tilde{Q}_{B,p} \quad (7)$$

(see Fig. 8). Since in this case $\tilde{Q}_{B,n} < 0$ the corresponding incremental delay:

$$\Delta\tau^* = -\frac{\tilde{Q}_{B,n}}{\tilde{J}_n(0)} \quad (8)$$

is positive and yields $\tau > t_d$, as shown in Fig. 9 for $x > 0.05 \mu\text{m}$. The image charge \tilde{Q}_C , instead, is still made of electrons leaving the collector edge, and thus gives a negative incremental contribution to $\tau(x)$ as in the low current case.

V. COLLECTOR DELAY

As a further application, we analyzed the collector current dependence of collector signal delay (τ_C). Fig. 10

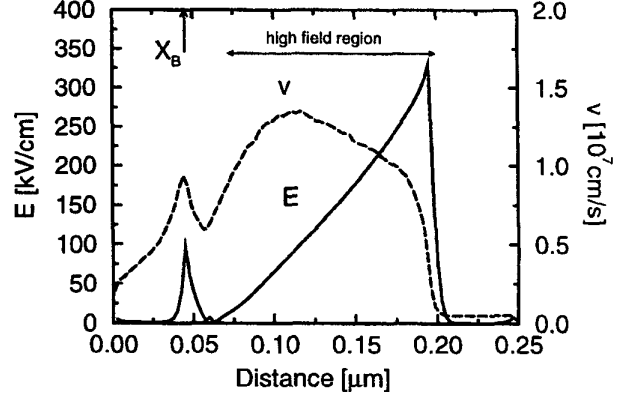


Fig. 7. Velocity and electric field profile of the BJT structure of Fig. 5 at high current $J_{n,0} = 4 \cdot 10^5 \text{ A/cm}^2$. Notice the existence of significant velocity overshoot ($v_{sat} = 9 \cdot 10^6 \text{ cm/s}$) in spite of the high bias current.

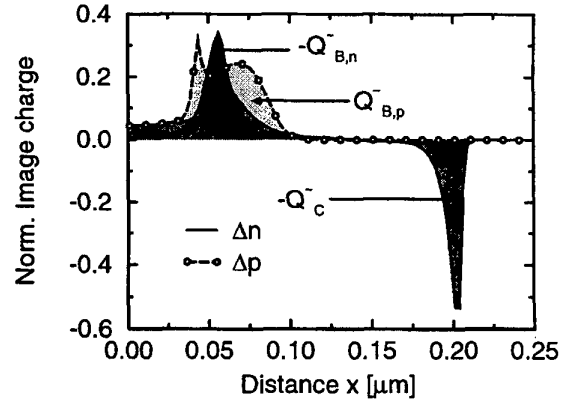


Fig. 8. Normalized electron and hole image charges induced by a Dirac's delta like electron pulse located at $x = 0.15 \mu\text{m}$ in the BJT of Fig. 5. The area below the curves is proportional to $\tilde{Q}_{B,p}$, $\tilde{Q}_{B,n}$ and \tilde{Q}_C , respectively.

shows that $\tau_C = \tau(X_C) - \tau(X_B)$ from Monte Carlo simulations (filled triangles) increases at high current, because of the increase of the extra delay $\Delta\tau^*$.

Due to a non-uniform velocity that even exceeds v_{sat} , the well known expression:

$$\tau_C = \frac{(X_C - X_B)}{2v_{sat}} \quad (9)$$

is not applicable. Thus, we compared our method with the τ_C formula of [2]:

$$\tau_C = \int_{X_B}^{X_C} \frac{(X_C - x)}{(X_C - X_B) v(x)} dx \quad (10)$$

that generalizes the simple expression above to a space-dependent carrier velocity, $v(x)$. Clearly, Eq.10 exhibits a

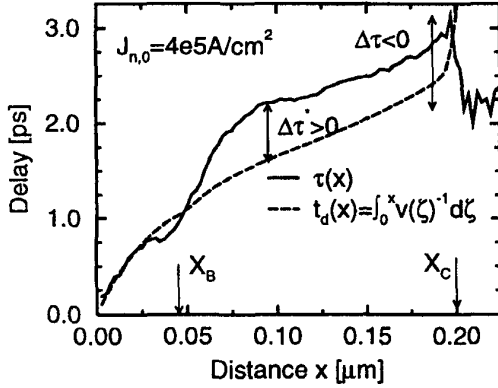


Fig. 9. Solid line: signal delay in the BJT structure of Fig. 5 computed with the self-consistent procedure. Dashed line: transit time of the same structure computed from the velocity profile of Fig. 7. Bias current $J_{n,0} = 4 \cdot 10^5$ A/cm².

much weaker current dependence (Δ in Fig. 10). This is because Eq. 10 assumes a stationary velocity profile (i.e. $\tilde{v}(x) = 0$). Due to high injection conditions, this assumption is verified only within the narrow high field region. Indeed, if τ_C is computed limiting the integration of Eq. 10 only to the high field region good agreement with the corresponding Monte Carlo result is obtained (compare \circ with \bullet in Fig. 10). This makes it clear that at high current the validity of Eq. 10 is limited to the high field portion of the epi collector.

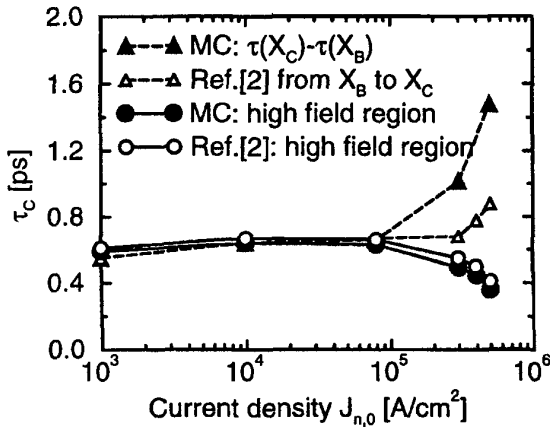


Fig. 10. Collector signal delay computed according to Eq. 10 and with the method of this work between X_B and X_C (dashed lines) and through the high field region (solid line).

VI. CONCLUSION

In summary, a new Monte Carlo procedure has been developed to study BJT signal delays in presence of strong non-equilibrium transport effects and up to high currents. The method was tested on advanced BJT designs, and allows users to clarify the physical meaning and the limitations of simplified delay expressions as, e.g., that of [2].

REFERENCES

- [1] E.F.Crabbè, J.M.C.Stork, G.Baccarani, M.V.Fischetti, and S.E.Laux, "The Impact of Non-equilibrium Transport on Breakdown and Transit Time in Bipolar Transistors," in *IEDM Technical Digest*, p. 463, 1990.
- [2] S.Laux and W.Lee, "Collector Signal Delay in the Presence of Velocity Overshoot," *IEEE Electron Device Letters*, vol. 11, no. 4, p. 174, 1990.
- [3] A.Das and M.Lundstrom, "Does Velocity Overshoot Reduce Collector Delay Time in AlGaAs/GaAs HBT's?," *IEEE Electron Device Letters*, vol. 12, no. 6, p. 335, 1991.
- [4] D.Chen, E.Sangiorgi, M.R.Pinto, E.C.Kan, U.Ravaioli, and R.W.Dutton, "Analysis of spurious velocity overshoot in hydrodynamic simulations," in *4th Workshop on Numerical Modeling of Processes and Devices for Integrated Circuits - NUPAD IV*, p. 109, 1992.
- [5] P.Graf, S.Keith, and B.Meinerzhagen, "Evaluation of Solenoidal and Statistically Enhanced Total Current Densities in Multi-Particle Monte Carlo Device Simulators," in *Proc.SISPAD*, p. 221, 1997.
- [6] B.Heinemann, K.E.Ehwald, P.Schley, G.Fischer, F.Herzel, D.Knoll, T.Morgenstern, W.Röpke, and W.Winkler, "Collector Profile Design of SiGe-HBTs for Optimized Static and High Frequency Performance," in *Proc.European Solid State Device Res.Conf.*, 1995.
- [7] A.Schüppen, U.Erben, A.Gruhle, H.Kibbel, H.Schumacher, and U.König, "Enhanced SiGe Heterojunction Bipolar Transistors with 160 GHz- f_{max} ," in *IEDM Technical Digest*, p. 743, 1995.
- [8] P.Palestri, C.Fiegna, L.Selmi, G.A.M.Hurkx, J.W.Slotboom, and E.Sangiorgi, "Optimization Guidelines for Epitaxial Collectors of Advanced BJT's with Improved Breakdown Voltage and Speed," in *IEDM Technical Digest*, p. 741, 1998.
- [9] P.Palestri, C.Fiegna, and L. aR.Bez, "A Better Insight in the performance of Silicon BJTs with Highly Non-Uniform Collector Doping Profile," *IEEE Trans.on Electron Devices*, vol. 47, no. 5, 2000.
- [10] W.Shockley, "Currents to Conductors Induced by a Moving Point Charge," *Journal of Applied Physics*, vol. 9, p. 635, 1938.
- [11] S.Ramo, "Currents Induced by Electron Motion," *Proc.IRE*, p. 584, 1939.
- [12] G.A.M.Hurkx, "Bipolar Transistor Physics," in *Bipolar and Bipolar-MOS Integration* (P.A.H.Hart, ed.), ch. 3, p. 73, Elsevier, 1994.